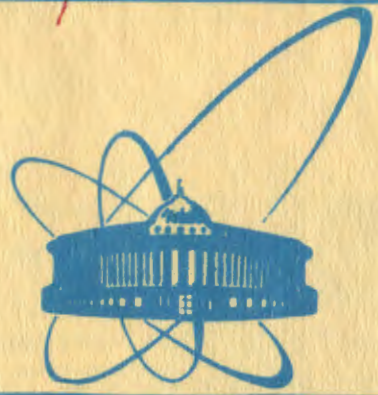

сообщения
объединенного
института
ядерных
исследований
дубна

E1-81-781

Z.Strugalski, K.Miller*

NEUTRON-PROTON RATIO DETERMINATION IN THE ATOMIC NUCLEUS PERIPHERY USING STRONGLY INTERACTING PROBES

* Institute of Physics of the Warsaw Technical University, Warsaw, Poland.

1981

1. INTRODUCTION

Many aspects about the nuclear matter distribution are now so firmly established that it has been possible to use them in order to investigate other physical quantities. Our knowledge about the nuclear matter distribution based on results of many experiments[1-5] is substantial, but so is our ignorance. The proton distribution has a spherical core of almost constant density surrounded by a surface region in which the density decreases outwards to zero[1-5]. The indications are quite strong that the neutron distribution does not differ by much from the proton distribution and does not extend much beyond it[5,6]. But, there is inadequate direct evidence on the neutron distribution, and what there is, is not conclusive[7].

Nuclei, in particular those of relatively large mass number, $A \gtrsim 16$, can be treated as spherical objects consisting of protons and neutrons. But, a nucleus is a quantum mechanical system and thus is represented by a wave function. This in theory extends over all space, although in practice it is confined to a definite finite region. It is not, however, confined to as sharply a delimited region as is, for example, the ivory of a billiard ball. But, if the density of nuclear matter is sensibly uniform over a certain region and drops to zero in a second region which surrounds the first, and if the thickness of this transition region is small compared with the linear dimensions of the first region, then something of nuclear radius exists[5]. This is expressed quantitatively in the following manner. The nuclear matter density distribution is characterized by the so-called half-way radius c, which gives the distance from the centre at which the density has dropped to half its maximum value and a surface thickness s, which has been defined as the distance over which the density drops from 90% to 10% of its maximum value[5].

The evidence, as concerns the proton density distribution, is the clearest one in the surface region and established with considerable accuracy the maximum density, the thickness of the surface region and the radial distance at which the density has fallen to half its maximum value. It is less clear in the interior, where the possibility of a slight change of the density towards the centre of the nucleus cannot be excluded[5]. From

the capture of K^- mesons it follows some tentative evidence that the nuclear matter distribution extends substantially beyond the kind of distance that is usually associated with the nuclear radius [8,9].

More experimental investigations are desired, therefore, which will tell us as much and more about the neutrons in the nucleus. Many techniques which have been used in such experiments necessarily involve strongly interacting probes, but it is extremely difficult to obtain model independent, quantitative information [7].

The aim of this work is: a) To show how it is possible to determine, in a model-independent manner, the ratio between the number N_n of the neutrons and the number N_p of the protons, N_n/N_p, in the peripheral region of the nucleus using strongly interacting probes; as peripheral we will treat the region of the radius $r \geq c+s/2$. b) To determine the ratio N_n/N_p in this region of the xenon nucleus.

The electrically charged pions serve here as the strongly interacting probes, but our considerations are valid as well when other electrically charged hadrons shall be applied.

An experimental information about the neutron-proton ratio in the peripheral region may throw the light at the question of the radial dependence of this ratio in the atomic nucleus as a whole; it is a question whose answer is difficult to find immediately for the present.

2. METHOD

Three facts form the basis of the method of the neutron-proton ratio determination in the atomic nucleus periphery. We express them first as the statements and we present later on, in Appendices, appropriate experimental argumentation. The facts in question are: a) High energy hadron, to say of the kinetic energy above 2 GeV, traversing an atomic nucleus undergoes two-body collisions with single nucleons met along its course in nuclear matter (Appendix 1); in particular, the collisions leading to the particle production are of such a kind. In result of such a hadron-nucleus collision nucleons, in particular the simply observed protons, and nuclear fragments are emitted and particles may be created. b) The hadron-nucleus collision events accompanied by 0 or 1 secondary proton are those in which the projectile collided with a nucleon in the peripheral region of the target-nucleus, i.e., those with the impact parameter $b \geq c + s/2$ (Appendix 2). c) The hadron-nucleon collisions in nuclei obey the electric charge conservation law.

In the light of these facts the principle of action of the method is simple. Let us suppose that we are able to detect all ionizing secondaries in any hadron-nucleus collision with 0 and 1 emitted protons. If, in result of the collision of a negative electric charge hadron with a target-nucleus, one observes 0, 2, 4, 6,..., i.e., an even number ionizing secondaries, it means that this hadron collided with a proton inside the target; if, in result of the collision, one observes 1,3,5,7,..., i.e., odd ionizing secondaries, it means that this hadron collided with a neutron inside the target. For example:

$\pi^- + p$ 0, 2, 4, 6,... ionizing secondaries (1)

$\pi^- + n$ 1, 3, 5, 7,... ionizing secondaries (1')

If, in result of the collision of a positive electric charge hadron with a target-nucleus, one observes 2,4,6,..., i.e., even ionizing secondaries, it means that this hadron collided with a proton inside the target; if, in result of the collision, one observes 1,3,5,..., i.e., odd ionizing secondaries, it means that this hadron collided with a neutron inside the target. For example:

$\pi^+ + p$ 2,4,6,... ionizing secondaries (2)

$\pi^+ + n$ 1,3,5,... ionizing secondaries (2')

In general: if an electrically charged hadron collides with a target-nucleus and an even number of ionizing secondaries is observed,we can state that this hadron collided with a proton inside the peripheral region of the target;if, in result of this collision, an odd number of ionizing secondaries appeared, we can state that this hadron collided there with a neutron.

The relation between the number N_0 of observed hadron-nucleus collision events with odd numbers of ionizing secondaries and the number N_e of the observed events with even numbers of ionizing secondaries is related simply to the neutron-proton ratio N_n/N_p inside the target-nucleus region where the hadron-nucleus collisions take place:

$$k = N_n/N_p = \kappa \cdot N_0/N_e , \qquad (3)$$

where κ is the coefficient accounting a possible energy-dependent difference in the values of the hadron-neutron and hadron-proton collision cross-sections. Denoting the hadron-neutron cross-section by σ_{hn} and the hadron-proton by σ_{hp}, we

can write:

$$k = N_n / N_p = \kappa N_0 / N_e = \sigma_{hp} / \sigma_{hn} \cdot N_0 / N_e \,. \qquad (3')$$

The values of appropriate hadron-proton collision cross-sections were measured in many experiments and are available from the CERN-HERA tables[10], for example. Some values of appropriate hadron-neutron cross-sections are known as well, but many are missing, however. The values for the hadron-neutron cross-sections can be evaluated nevertheless, from the commonly known relations between σ_{hn} and σ_{hp} cross-sections[11,12]. For example, for the pion-nucleon collisions there are: $\sigma(\pi^+ + n) = \sigma(\pi^- + p)$, $\sigma(\pi^- + n) = \sigma(\pi^+ + p)$.

The hadron-nucleus collisions with 0 and 1 secondary proton can be, in principle, singled out simply in many experiments performed using the bubble chambers and electronic techniques. The numbers N_0 and N_e of the hadron-nucleus collision events with 0 and 1 secondary proton and an odd and an even number of ionizing secondaries can be determined without difficulties as well. The experimental problem arises, however: how it is possible to record and detect all the charged secondaries in an event, using the now existing experimental techniques; this question is a subject matter of Appendix 3.

The method, presented above, differs by much from that worked out by one of authors (Z.S.) about fifteen years ago[6]. It is much handed and provides more accurate results, without involving any corrections into experimental data on the N_0 and N_e quantities in formula (3').

3. NEUTRON-PROTON RATIO DETERMINATION IN THE PERIPHERAL REGION OF THE XENON NUCLEUS

The problem to be discussed now in this section is concerned with the experimental determination of the N_n/N_p ratio in the peripheral region of the xenon nucleus. In order to determine this quantity, let us use the photographs of the 26 litre xenon bubble chamber[13] of the JINR, Dubna, exposed to the beam of positively charged pions of 2.34 GeV/c momentum and of negatively charged pion beams of 5 and 9 GeV/c momenta, and photographs of the 180 litre xenon bubble chamber[14] of the ITEPh, Moscow, irradiated in the negatively charged pion beam of 3.5 GeV/c momentum.

3.1. The Xenon Bubble Chambers

Both the chambers are of rectangular parallelepipedal volume; the smaller of 55·29.5·16 cm^3, the bigger one of 104·.40·40 cm^3. Both are photographed through the top plexiglass wall of 55·29.5 cm^2 and 104·40 cm^2, correspondingly; the smaller, by two cameras; the bigger one, by three cameras. The lens axes are parallel one to another and perpendicular to the top wall of the chamber. The illumination by the light impulses comes from the side, perpendicular to the lens axes. The spatial resolution of a bubble location is $\pm\Delta X = \pm\Delta Y = 0.2$ mm, $\pm\Delta Z = 0.5$ mm for both the chambers. They work without magnetic field.

3.2. Beam and Exposure

No more than five pions were introduced into the chambers during the exposure impuls, coaxially along their lengths. The beam pion tracks were parallel and spaced within distance limits of a few centimeters from the chamber axis.

3.3. Scanning and Measurements

The photographs were scanned and rescanned for the pion-xenon nucleus collision events which could occur in a chosen parallelepipedal region of 42·10·10 cm^3 in the bigger chamber and within the region of 27·14·5 cm^3 in the smaller one, both centered inside the chambers. Any sharp change in the straight line track of any beam pion was accepted to be an indication that this pion has undergone the interaction with a xenon nucleus. The end or deflection points of any beam pion track were accepted to be the pion-xenon nucleus collision location. In fact we are able to detect the collision events in which the beam pion track ends off forming a "star" or not or deflects at an angle no less than 2 degrees, in accompaniment or not by any number of negaton-positon pairs produced by gamma quanta looking as coming from the collision place.

The secondary neutral pions of any kinetic energy, including zero, are recorded and identified in our chambers by the well visible tracks of the negaton-positon pairs and electron-photon showers created by the gamma quanty appearing in the neutral pion decays. The minimum energy of the gamma quanta detected with a constant efficiency being about 100% is roughly 5 MeV. The positive pions stopping within the chamber are identified simply by the characteristic track sequence left by the charged secondaries arising in the decay process. Some dif-

ficulties have been met in attempts to identify the negatively charged pions, when left a small-length-tracks or when left the tracks as particles gone out of the chamber; it is difficult to distinguish them from the protons of similar tracks. If the scanning is limited to the collision events with 0 and 1 proton track this difficulty is partly eliminated because of a better track resolution in the collision events with small number of tracks[6]. Stopping kaons are identified without difficulties as well. Similarly, it was possible to identify hyperons, if decayed inside the chamber. The neutrons which are emitted in a collision process interact with the xenon nuclei frequently leaving characteristic "neutral stars". The evaporated protons, of energies much smaller than about 20 MeV, and the emitted heavier fragments of the target-nucleus leave tracks of the length evidently smaller than 5 mm.

Tracks of the lengths larger than 5 mm are visible well in any of the pion-xenon nucleus collision events and are detectable with a constant efficiency of nearly 100% in both the chambers. To this minimum length corresponds the minimum kinetic energy of the protons of 20 MeV and of the charged pions or roughly 10 MeV. The tracks of the smaller lengths are visible as well but in this case the detection efficiency is not constant in events with various numbers of secondaries.

All tracks left by the particles stopping inside the chamber without visible interaction or decay are accepted to be the proton-tracks, the rest of tracks are accepted to be left by the pions. The portion of the pion-left-tracks in the sample of tracks accepted as left by protons, in all the pion-xenon nucleus collision events singled out in the scanning, is estimated to be no more than 2%; the portion of the pion-left-tracks in the one-proton events is much smaller, being, as estimated, much less than 0.5%.

The protons of kinetic energy from 15 up to about 220 MeV, the secondary pions: the negatively charged of kinetic energy from about 10 up to 150 MeV, the positively charged of kinetic energy from 0 up to about 150 MeV, and the neutral pions of any kinetic energy, including zero MeV, are recorded and identified with the efficiency being near to 100% within the total 4π solid angle in the 180 litre chamber; in the 26 litre chamber such registration and identification efficiency is for the protons of kinetic energy from 15 to about 115 MeV, for negative electric charge pions of kinetic energy from 10 up to about 60 MeV, for the positive charge pions from 0 up to 60 MeV, and for the neutral pions of any kinetic energy, including zero MeV. We have estimated that

roughly over 90% of emitted protons are stopping inside the 180 litre chamber.

The scanning efficiency for all the pion-xenon nucleus collision events registered in our experiments were better than 99%.

It is possible to measure the kinetic energy of the stopping protons and of the stopping positive charge pions,using the range-energy relation. The accuracy of the energy measurement is, in average, 4% for the protons and for the electric charged pions. The emission angles of the protons and of the charged and neutral pions can be estimated as well. The accuracy is, in average, 2 degrees for the protons and 1 degree for the pions - both electrically charged and neutral.

3.4. Experimental Data

A total of about 43000 pion-xenon collision events of any type has been found in about 65000 stereophotographs, the number of 2882 collision events with zero and one proton has been observed in them. General characteristic of the experimental material is given in table 1.

Table 1

The characteristics of the pion-xenon nucleus collision samples. Denotations: R - reaction type, P_π - incident pion momentum in GeV/c, N_p - number of photographs scanned, N_a - number of collision events of any kind, $N_0 = N(Pi+n)$ and $N_e = N(Pi+p)$ - numbers of the pion-neutron and the pion-proton collision events in the sample of the pion-xenon collision events with 0 or 1 emitted proton correspondingly

R	P_π	N_p	N_a	N_o	N_e
$Pi^+ + Xe$	2.34	30000	20000	1083	564
$Pi^- + Xe$	3.50	10000	8000	251	190
$Pi^- + Xe$	5.00	10000	6000	180	138
$Pi^- + Xe$	9.00	15000	9000	298	178

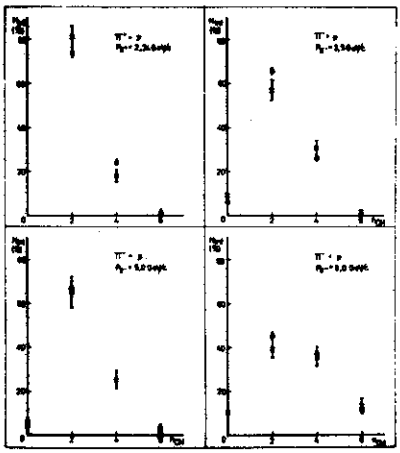

Fig.1. The distributions of the charged secondary multiplicity n_{CH}: x - in the pion-xenon nucleus collision events with one emitted proton; Δ - in the elementary pion-proton collision events /10/.

Due to the acceptation of the low limit value for the deflection angles of the pions in one-prong collision events with zero secondary protons and in two-prong collision events with one secondary proton, being $\theta_\pi \geq 5$ degrees, we preserve the same detection efficiency for both the classes of events with one secondary pion; in such classes of events the scanning efficiencies could be different, when smaller deflection angles would be taken into account.

In order to test the correctness of our selection procedure, let us compare the charged secondary multiplicity distribution in our sample of events with one secondary proton, accepted to be the quasielementary collision events, with corresponding charged secondary multiplicity distribution in the elementary pion-proton collisions at the same value of the incident pion momentum. The charged secondary multiplicity distribution in elementary pion-proton collisions has been prepared using the existing data on corresponding cross-sections for 0,2,4,6,... prong events /10/. Result is presented in fig.1. It should be concluded that both the distributions, that for the events selected in the pion-xenon nucleus collisions and that for the elementary pion-proton collisions, are identical. We can treat, therefore, the events with zero secondary protons, per analogy, as correctly selected pion-neutron collision events, as well.

Then, the numbers N_0 and N_e determined in our experiment, table 1, can be used in formula (3') for the N_n/N_p ratio determination.

Now, the difference in the cross-sections for the pion-proton and the pion-neutron elementary collisions, contained in formula (3') as the coefficient $\kappa = \sigma_{\pi p}/\sigma_{\pi n}$, should be evaluated, at those values of the incident pion momenta which have been used in our experiment. Appropriate values for the $Pi^+ + p$ and $Pi^- + p$ collision cross-sections are taken from the CERN-HERA tables /10/, those for corresponding $Pi^+ + n$ and $Pi^- + n$ col-

Table 2

The total cross-sections for the pion-proton [10] and the pion-neutron collisions. Denotations: P_π - the incident pion momentum in GeV/c, q - the electric charge of the incident pion, $\sigma_{\pi p} = \sigma(\pi + p)$ and $\sigma_{\pi n} = \sigma(\pi + n)$ - total cross-sections for the pion-proton and pion-neutron collisions in mb, $\kappa = \sigma(\pi+p)/\sigma(\pi+n)$.

P_π	q	$\sigma_{\pi p}$	$\sigma_{\pi n}$	κ
2.34	+	30.8900 ± 0.2700	34.6300 ± 0.2900	0.89 ± 0.02
3.50	-	31.5690 ± 0.0150	28.2240 ± 0.0150	1.12 ± 0.001
5.00	-	28.5800 ± 0.2000	26.4900 ± 0.2000	1.07 ± 0.012
9.00	-	25.0000 ± 4.0000	25.0000 ± 4.0000	1.00

lisions were calculated using the relations [11,12] written on pahe 4. The values of corresponding cross-sections are given in table 2, where the values of the coefficient κ are presented too.

All the quantities are available now for the $k = N_n/N_p$ ratio determination using formula (3′).

3.5. Result

The values of the neutron-proton ratio, $k = N_n/N_p$, evaluated on the basis of various samples of the pion-xenon nucleus collision events are written in table 3. They are independent of the incident pion momentum, and we present the average value being the result of our measurement: $k = 1.52 \pm 0.12$.

The same sample of experimental data, table 1, we have used for determination of the ratio k applying the different method, which has been described in detail by one of us [6], and we found not necessary to present it here once again. It provided the value for this ratio $k = 1.51 \pm 0.12$. Both the methods provide independent results. We have, then, the average value for the neutron-proton ratio in the peripheral region of the xenon nucleus:

$$k = N_n/N_p = 1.52 \pm 0.08. \qquad (4)$$

Table 3

Neutron-proton ratio k in the peripheral region of the xenon nucleus, measured using various samples of the pion-xenon nucleus collision events. Denotations as in tables 1 and 2.

R	P_{π}	N_o/N_e	κ	$k = \kappa \cdot N_o/N_e$
$Pi^+ + Xe$	2.34	1.74 ± 0.19	0.89 ± 0.02	1.55 ± 0.18
$Pi^- + Xe$	3.50	1.27 ± 0.29	1.12 ± 0.001	1.47 ± 0.32
$Pi^- + Xe$	5.00	1.41 ± 0.29	1.07 ± 0.012	1.51 ± 0.32
$Pi^- + Xe$	9.00	1.65 ± 0.21	1.00	1.65 ± 0.21

The neutron-proton ratio for the xenon nucleus as a whole is $k_1 = (A-Z)/Z = 1.43$. We can state, therefore: a) There is an excess of the neutrons in the peripheral region of the xenon nucleus, but it is, in average, no more than about 6% as the excess in this nucleus as a whole. b) It is reasonable to suspect now that the neutron-proton ratio is almost radial-independent inside the atomic nucleus, at least inside the xenon nucleus, being of the value near to the ratio $k_1 = (A-Z)/Z$.

4. CONCLUSIONS AND REMARKS

We have presented above the effective model-independent method of the neutron-proton ratio determination in the peripheral region of atomic nuclei. This method has been applied here in order to give an example rather, for one nucleus only, using the xenon bubble chambers.

We do not find necessary to argue that this method is just applicable in experiments with an electronic techniques as well. Obviously, there is a great deal for nuclear structure experimentalists to determine this way the neutron density differences in the peripheral region of many atomic nuclei.

It is not known at the present how it is possible to apply effectively similar method for an extraction directly of a precise information about the $k = N_n/N_p$ radial-dependence in the nuclear interior. Much difficulties are met in solving this problem in question. For example, such difficulties have been illustrated [15] in attempts to extract precise information about the nuclear interior from proton scattering at high energy.

APPENDIX

A.1. Quasielementary Hadron-Nucleon Collisions in Target-Nuclei

Let us present here the experimental facts on which the conclusion may be based that high energy hadrons, of over about 1 GeV, collide in the main with single nucleons inside the target-nucleus, in passing through it; in result of such collisions hadrons are deflected or the particles are created.

It is well known the linear dependence of the charged secondary multiplicity dispersion $D=\sqrt{\langle N^2\rangle-\langle N\rangle^2}$ on the mean multiplicity $\langle N\rangle$, in pion-nucleus collisions at energies from values of a few GeV up to the higher ones available now in accelerator experiments [16-18]. This dependence is almost the same as the straight line obtained as the best fit to the $D-\langle N\rangle$ dependence in the elementary pion-proton collisions[19]. Such coincidence of the $D-\langle N\rangle$ dependences can take place only when the observed distribution of the produced particle multiplicity in pion-nucleus collisions is a result of the outcome of the single elementary hadron-nucleon collisions inside the target-nucleus or if it is a result of the composition of the outcome in some number of such elementary collisions in the target[20]. In such a case only in pion-nucleus collisions the produced particle multiplicity distribution scales in the same way as in the pion-nucleon ones[21].

In addition, a direct confrontation of the charged secondary multiplicity distribution in the elementary pion-proton collisions with corresponding distribution in the pion-nucleus collisions accompanied by one emitted proton, at the same incident pion momentum, shows a coincidence of both these distributions, fig.1.

The above presented facts enable us to state that, in fact, the pion-nucleus collisions with no more than one emitted proton are the quasielementary pion-nucleon collisions. There are no any reasons to consider that all the hadron-nucleus collisions with no more than one secondary proton are of a different kind.

A.2. The Location of the Hadron-Nucleus Collisions with no More than One Emitted Proton Inside the Target-Nucleus

As is usually practiced, some functional dependences are assumed for a description of the experimentally known proton density radial distribution in nuclei with the mass number $A\gtrsim 16$; the so-called Fermi distribution[22], Helm distribution[23],

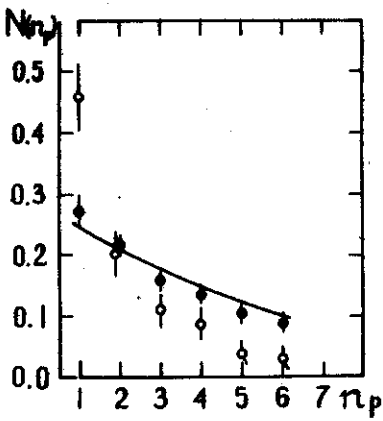

Fig.2. The distribution $N(n_p)$ of the pion-xenon nucleus collision events, at 3.5 GeV/c momentum, with various numbers n_p of emitted protons of kinetic energy larger than 20 MeV, full circles; corresponding distribution in the class of the pion-xenon nucleus collision events in which the incident pion undergoes the deflection only without particle production, open circles. Solid line - the calculated distribution of the collision impact parameters $W[b(n_p)]$, corresponding to various nuclear matter layer thicknesses in the xenon nucleus expressed in units of the number of protons n_p per the area of $\pi \cdot 1.81^2 fm^2$.

shell model distribution[24]. The only discrepancy between these distributions appears very close to the centre of the nucleus, where nothing is known about the distribution from the electron scattering results[5]. Each of these distributions is of the shape similar to that described qualitatively above, characterized by the half-way radius c and the surface thickness s.

It is actually possible to obtain a very good fit to the data for $A \gtrsim 16$ with two assumptions[5]: a) the surface thickness is constant at $a = 2.49$ f; b) the maximum nuclear matter density ρ_{max} is constant at $A \cdot \rho_{max} = 0.168$ fm^{-3}.

It is possible, using one of these distributions, to calculate the frequency $W[b(n_p)]$ to occur an impact parameter b to which definite nuclear matter layer thickness, measured in the number of protons per some area, corresponds. It has been done for various atomic nuclei using the Fermi distribution[25]. It turned out that the frequency distribution $W[b(n_p)]$ calculated this way for the xenon nucleus is almost the same as the distribution $N(n_p)$ of the numbers n_p of emitted protons, for $n_p \leq 6$, of kinetic energy above about 20 MeV in the pion-xenon collisions at 3.5 GeV/c momentum of incident pions[26], fig.2; to the number of emitted protons $n_p \leq 1$ corresponds, as it has been proved[25] the impact parameter $b \geq c + s/2$.

Moreover, the pion-xenon nucleus collision events were discovered, at 3.5 GeV/c momentum, in which incident pions undergo a deflection only in accompaniment by various numbers n_p of emitted protons without particle production[27]. The n_p-distri-

bution in such events is presented in fig.2 as well; this dependence decreases faster than the $N(n_p)$ for all the collision events and as the W(b).

We can see, therefore, that the pion-xenon nucleus collision events with no more than one emitted proton may be considered as taking place in the peripheral region of the target-nucleus.

The distribution $N(n_p)$ for a given target-nucleus is almost energy-independent and it changes not by much for various projectile-hadrons[28].

Then, it is reasonable to think that in general the hadron-nucleus collisions with one and zero protons emitted are such which take place in the peripheral region of the target-nucleus, i.e., at $b \gtrsim c + s/2$.

A.3. An Experimental Ability to Detect Effectively all the Charged Secondaries in Hadron-Nucleus Collision Events

Various ionizing secondaries can be detected in various detectors with various efficiency, smaller than 100%. For example, some ionizing particles do not leave visible tracks if of energy smaller than a definite; some of track-leaving-particle deflection angles are indetectable when smaller than of a definite minimum value, etc. In various types of collision events the detection efficiency may vary. Special analysis should be performed for each of detectors to be used for the N_n/N_p ratio determination in the peripheral region of the target-nuclei.

In this paper, in section 3, we have described shortly, as an example, such analysis for the xenon bubble chambers.

At the time, many of existing bubble and streamer chambers and electronic arrangements satisfy the conditions desired for the N_n/N_p ratio determination using them.

REFERENCES

1. Hofstadter R. Rev.Mod.Phys., 1956, 28, p.214.
2. Hofstadter R. Ann.Rev.Nucl.Sci., 1957, 7, p.231.
3. Hofstadter R. Nuclear and Nucleon Structure, Frontiers in Physics. W.A.Benjamin, New York, 1963.
4. Hofstadter R., Collard H.R. Nuclear Radii, Landolt-Bernstein Series, Group 1,2. Springer-Verlag, Heidelberg, 1967.
5. Elton L.R.B. Nuclear Sizes, Oxford University Press, 1961.

6. Strugalski Z. Nucl.Phys., 1966, 87, p.280.
7. Thomas A.W. Int. Conf. on Nucl.Phys. Berkeley, August, 1980. TRI-PP-80-22.
8. Burhop E.H.S. The Neutron Distribution in the Surface of Heavy Nuclei, London, 1965; Nucl.Phys., 1965, B1, p.483.
9. Bethe H.A., Siemens P.J. Nucl.Phys., 1970, B21, p.589.
10. Famino F. et al. CERN-HERA, 79-01, 79-02, 79-03, Geneva, 1979.
11. Shmushkiewich I.M. Doklady AN SSSR, 1955, 103, p.235.
12. Shmushkiewich I.M. Doklady AN SSSR, 1956, 106, p.801.
13. Kanarek T.I. et al. Proc. of the Int. Conf. on High Energy Accel. and Instr., CERN, 1959.
14. Kusnetsov E.V. et al. Instr. and Exp.Techn., 1970, 2, p.56.
15. Brissaud I., Campi X. Phys.Lett., 1979, 86B, p.141.
16. Busza W. In: High Energy Physics and Nucl.Struct., 1975, Santa-Fe and Los Alamos, AIP Conference Proc., No.26, p.211; Acta Phys.Pol., 1977, B8, p.333.
17. Abrosimov A.T. et al. Nucl.Phys., 1979, B158, p.11.
18. Vegni G. High Energy Interactions on Nuclei. In: Proc. Int.Conf. on High Energy Phys., Geneva, 1979, vol.2, p.582.
19. Wroblewski A. Proc. 8th Int.Symp. on Multipart. Dynamics, Kayserberg, 1977, p.37.
20. Strugalski Z. JINR, E1-81-154, E1-81-155, E1-81-156, Dubna, 1981.
21. Yule G.U., Kendall M.G. An Introduction to the Theory of Statistics, Charles Griffin, London, 1953.
22. Elton L.R.B., Hiley B.J., Price R. Proc.Phys.Soc., 1958, 73, p.112.
23. Helm R.H. Phys.Rev., 1956, 104, p.1466.
24. Fregean J.H. Phys.Rev., 1956, 104, p.225.
25. Strugalski Z., Pawlak T. JINR, E1-81-378, Dubna, 1981.
26. Strugalski Z. et al. JINR, E1-80-39, Dubna, 1980.
27. Strugalski Z. et al. JINR, E1-11975, Dubna, 1978.
28. Strugalski Z. JINR, E1-80-216, Dubna, 1980.

Received by Publishing Department
on December 9 1981.